Lateral Current Injection Distributed Feedback Laser with Wirelike Active Regions

Takahiko Shindo[1], Tadashi Okumura[2], Mitsuaki Futami[1], Ryo Osabe[1], Hitomi Ito[1],
Takayuki Koguchi[1], Tomohiro Amemiya[1,2], Nobuhiko Nishiyama[1], and Shigehisa Arai[1,2]

[1]*Department of Electrical and Electronic Engineering, Tokyo Institute of Technology*
[2]*Quantum Nanoelectronics Research Center, Tokyo Institute of Technology*
2-12-1-S9-5 O-okayama, Meguro-ku, Tokyo 152-8552, Japan
E-Mail shindou.t.aa@m.titech.ac.jp

Abstract

One of the promising candidates to solve a problem of a performance limitation of LSI is replacing the electrical global wiring by an on chip optical interconnection. A semiconductor membrane laser, which consists of a high-index contrast waveguide, is expected to operate with ultra low threshold current due to an enhanced modal gain. We have introduced a lateral current injection (LCI) structure for electrically pumped membrane laser, and demonstrate LCI type Distributed feedback (DFB) laser with wirelike active region prepared on a semi-insulating (SI) InP substrate. A threshold current of as low as 11 mA and a stable single-mode operation were obtained for a device with the stripe width of 1.5 μm and the cavity length of 300 μm under a room-temperature continuous-wave (RT-CW) condition.

I. INTRODUCTION

It is predicted that the progress of the processing speed and integration of large scale integrated (LSI) circuits will soon confront limitation associated with RC delay and large power dissipation in the electrical interconnection. As one of promising approaches for solving this problem, an introduction of the optical interconnection instead of electrical wiring has been extensively studied [1,2]. In optical devices for short-distance optical communication systems, low power dissipation and compactness carry significant weight compared with conventional optical devices. Especially, in semiconductor light sources for on-chip optical interconnections, the available power dissipation for the semiconductor laser is estimated to be less than 100 fJ/bit [2]. Therefore, ultra-low threshold current operation is strongly required. The low power dissipation of 8.76 fJ/bit has been reported with a semiconductor laser using photonic crystal structure under optical pumping [3]. However, the operation with electrical pumping has not been realized yet.

For low threshold current semiconductor light sources, microdisk lasers [4] or photonic crystal lasers [5,6] have been reported. However these devices have some disadvantage such as low output efficiency or large resistance. Alternatively, we have been investigating a semiconductor membrane laser which has a thin semiconductor core layer and low refractive-index cladding layers such as SiO_2 or BCB [7]. Previously, we demonstrated an optically pumped membrane laser with low threshold pump power of 0.34 mW [8]. In addition, to realize a current injection type membrane laser, we introduced a lateral current injection (LCI) structure [9] and demonstrated LCI Fabry-Perot lasers [10,11] as well as DFB lasers [12,13] fabricated on a SI-InP substrate. In this study, we introduced a wirelike active region structure to the LCI-DFB laser, since low threshold current operation can be expected due to its small active region volume and strong index-coupling effect [14]. In addition, enhancement of the carrier injection efficiency was theoretically expected by introduction of etched active regions to LCI structure [15].

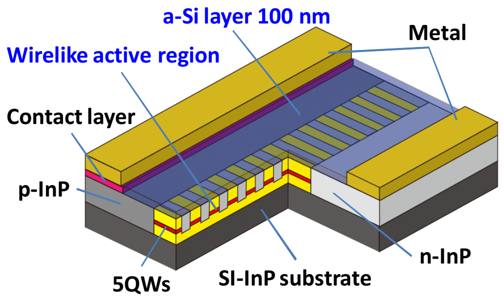

Fig. 1 Schematic structure of the LCI-DFB laser with wirelike active regions.

II. DESIGN AND FABRICATION

Figure 1 shows the schematic structure of the LCI-DFB laser with wirelike active regions. Firstly, we calculated the threshold current dependence on the cavity length, as shown in Fig. 2. The calculated structures were the LCI-DFB laser with wirelike active regions and that with a-Si surface grating [13], where the depth of the surface grating formed on the top of the laser stripe was assumed to be 100 nm. The active region was assumed to be consisting of 5 quantum-wells (5QWs) in both cases. Hence the optical confinement factor in the active region is about 5.6% in both cases. The refractive-index of the a-Si was assumed to be 3.45. On the other hand, in the LCI-DFB laser with wirelike active regions, the grating structure was assumed to be active region periodically

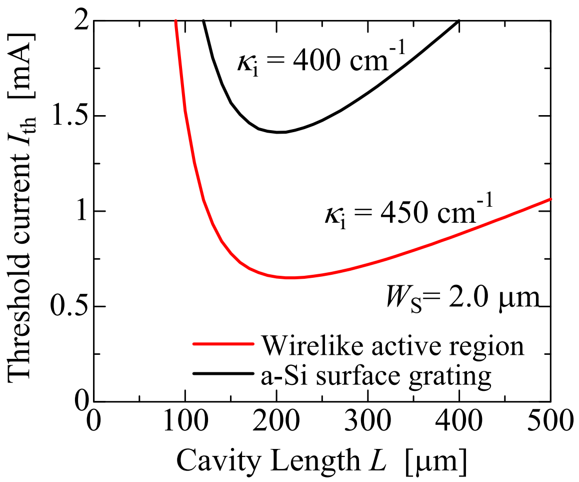

Fig. 2 Calculated threshold current dependence on the cavity length.

etched and filled with InP. In addition, to keep the optical confinement factor in 5QWs almost the same as that in the above mentioned LCI-DFB laser with a-Si surface grating, a 100 nm-thick a-Si layer was assumed to be formed on the top of the laser stripe. In these structures, the total GaInAsP layer thickness and the stripe width were 400 nm and 2.0 μm, respectively. From the calculation result, an index-coupling coefficient in the grating of wirelike active region structure and that of a-Si surface grating structure were obtained to be 400 cm^{-1} and 450 cm^{-1}, respectively. As can be seen in Fig. 2, by introducing the wirelike active region structure, the threshold current can be reduced to be about 0.5 mA due to an effect of the high index-coupling coefficient and the reduction of the active region volume. Please note the internal quantum efficiency in this calculation was 100%.

An initial wafer of the fabricated LCI-DFB laser with wirelike active regions consisted of undoped GaInAsP core layer was prepared on an Fe doped SI-InP by organo-metallic vapour-phase-epitaxy (OMVPE) method; the core layer included an undoped-GaInAsP lower optical confinement layer (OCL, λ_g = 1.2 μm, 140 nm thick) and five 1% compressively-strained (CS) $Ga_{0.22}In_{0.78}As_{0.81}P_{0.19}$ QWs (6-nm-thick well) with -0.15% tensile-strained (TS) $Ga_{0.25}In_{0.75}As_{0.50}P_{0.50}$ barriers (10 nm), an upper GaInAsP OCL (λ_g = 1.2 μm, 140 nm thick), and undoped thin i-InP layer. First, an electron-beam-lithography (EBL) was carried out to form wirelike active regions. After grating patterns were transferred to SiO_2 mask by CF_4 reactive-ion-etching (RIE), active layers were completely etched by CH_4/H_2 RIE. Then a wet cleaning process was applied to remove the damaged layer by dry etching, and undoped InP was regrown into the groove regions. Next, the LCI structure was formed by CH_4/H_2 RIE and two-step OMVPE selective regrowth process. After formation of the mesa stripe structure with a width of 7 μm and a height of 400 nm by CH_4/H_2 RIE, n-InP (N_D = 4 × 10^{18}/cm^3) was selectively regrown on the both sides of the mesa structure as a cladding layer. Then, by etching a part of the 7 μm wide active region stripe and embedded n-type InP layer by the similar manner, narrow stripe (1.5 μm) was formed. After that, p-InP (N_A= 4 × 10^{18}/cm^3) and p-GaInAs (N_A = 8 × 10^{18}/cm^3) were regrown by the same way and a part of GaInAs contact layer near the stripe edge was removed by wet chemical etching to reduce the optical absorption loss in the GaInAs contact layer. Then Ti/Au electrodes were evaporated on the n-InP and p-InP regions. Finally, a 100 nm a-Si layer was deposited on the laser stripe by P-CVD.

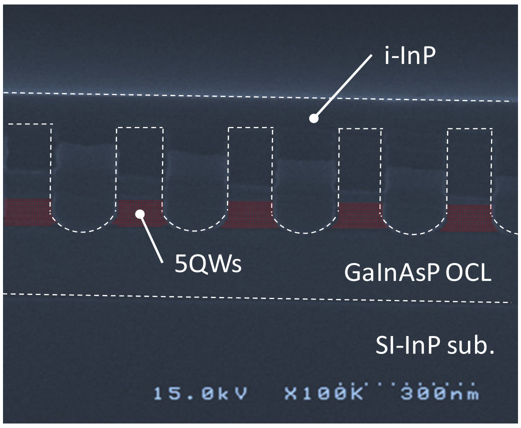

Fig. 3 Cross sectional SEM view of the wirelike active region after regrowth process.

Since the fabricated LCI-laser on a SI-InP layer has an asymmetric structrure in the vertical direction, an optical mode field in the core layer leaks to the SI-InP lower cladding due to relatively thin GaInAsP OCL especially in the groove regions. To prevent large waveguide loss due to this leaky optical mode field in groove regions, an a-Si layer was deposited so as to confine the optical mode field in the core layer.

Figure 3 shows the cross sectional SEM view of the wirelike active regions. The period and wire width were designed to be 100 nm and 242.5 nm, respectively. As can be seen in Fig. 4, the groove regions are filled with undoped InP and almost flat top surface was obtained.

III. EXPERIMENTAL RESULT

The light output and voltage-current characteristics of the fabricated device are shown in Fig. 4. The cavity length and the stripe width were 300 μm and 1.5 μm, respectively. As can be seen, the threshold current (I_{th}) of 11 mA, and an external differential quantum efficiency from the front facet (η_{df}) of 26% were obtained under a RT-CW condition. The differential series resistance and the voltage at the threshold current were around 68 Ω and 1.7 V, respectively. The threshold current of this device was not low compared with our typical LCI-type lasers fabricated on a SI-InP substrate [11]. Then, from the calculation result shown in Fig. 2, one order lower threshold current was estimated. One of the reasons is low internal quantum efficiency in this device. From our LCI FP laser results, the estimated internal quantum efficiency is about 40%, which should be improved by the

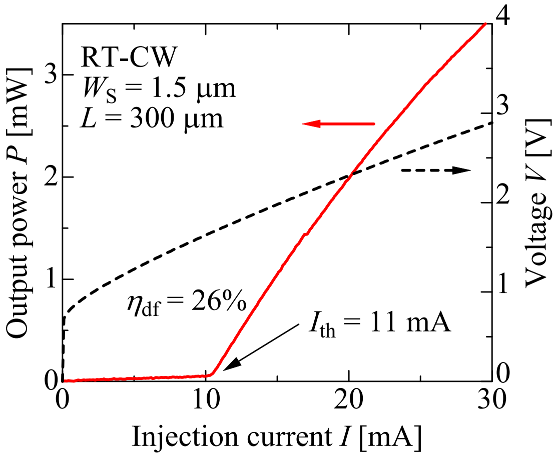

Fig. 4 Lasing characteristics of the LCI-DFB laser with wirelike active regions.

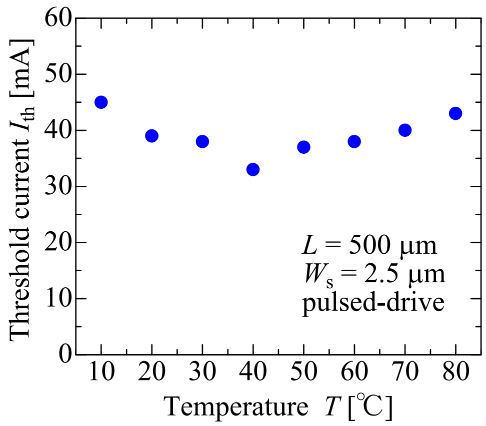

Fig. 5 Temperature dependence of the threshold current of the LCI-DFB laser with wirelike active regions.

modification of the active region structure. Another reason for the high threshold current of the fabricated device compared with the calculated result is the largely detuned lasing wavelength.

Figure 5 shows the temperature dependence of threshold current of another sample under a pulsed condition. As can be seen, the threshold current took the minimum value of 33 mA at 40 °C. Hence the Bragg wavelength is considered to be 8-10 nm longer than the gain peak wavelength at around 20 °C.

Figure 6 (a) shows the differential series resistance dependence on the stripe width of the LCI-DFB laser with wirelike active regions (Wirelike) and that of the LCI quantum-well laser (Film) fabricated on the same wafer. The y-intercept, which can be regarded as the contact resistance between the metal electrodes and p-GaInAs and n-InP contact layers, was measured to be around 30 Ω for both samples, the evaporation of Ti/Au electrodes can be attributed to these poor series resistances. From Fig. 6 (a), the differential series resistance of the LCI laser with wirelike active regions (R_{wirelike}) is 1.7 times larger than that of LCI quantum-well (R_{film}). But, the area of GaInAsP region of wirelike active regions (S_{wirelike}) is no more than

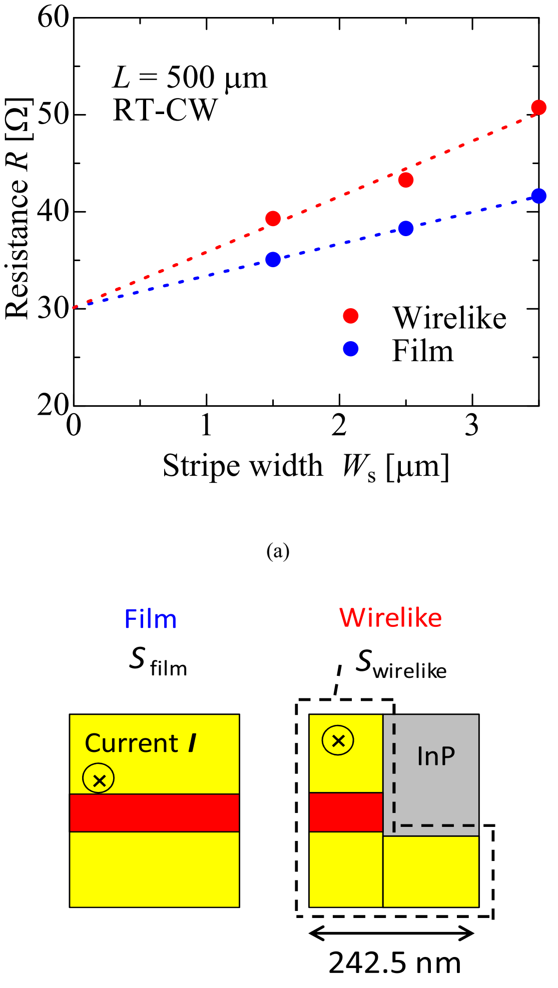

(a)

(b)

Fig. 6 (a) Differential series resistance and (b) compariosn of the structures of the LCI-FP laser and LCI-DFB laser with wirelike active regions.

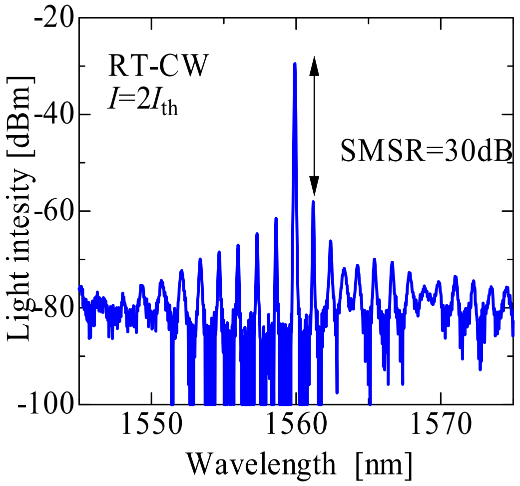

Fig. 7 Lasing spectrum of the LCI-DFB laser with wirelike active regions.

1.5 times smaller than that of quantum-well structure (S_{film}) as can be seen in Fig. 6 (b). Therefore, almost all current seems to flow in GaInAsP layer (OCLs and active regions) and leak current in regrown InP layer can be negligible.

Figure 7 shows the lasing spectrum of the LCI-DFB laser with wirelike active regions for the cavity length of 300 μm and the stripe width of 1.5 μm. Even though a clear stopband attributed to the DFB structure cannot be confirmed and the resonant mode spacing near the lasing wavelength was approximately 1.3 nm for the cavity length of 300 μm, the effective refractive-index (group index) of the waveguide can be estimated to be 3.12 which is slightly smaller than that of conventional buried heterostructure laser because an optical field slightly penetrates in the low refractive-index region. Since the sub-mode suppression-ratio (SMSR) of 30 dB was obtained at a bias current of two times the threshold, this device is operating with a DFB mode.

IV. CONCLUSION

A step toward a realization of an electrically driven LCI-DFB laser for on-chip optical interconnection, we investigated the LCI-DFB laser with wirelike active regions on a SI-InP substrate. From the theoretical study, the threshold current of LCI-DFB laser with wirelike active regions was confirmed to be advantageous than that with flat quantum-wells due to the volume effect of the active region. From the experimental study of the LCI-DFB laser with 5 layered wirelike active regions with 100 nm width in the period of 242.5 nm, a threshold current of 11 mA and a differential quantum efficiency of 26% from the front face were obtained for the cavity length of 300 μm and stripe width of 1.5 μm.

ACKNOWLEDGEMENT

This research was financially supported by Grants-in-Aid for Scientific Research (#1900200 9, #22360138, #21226010, #08J55211, #10J08973) from the Ministry of Education, Culture, Sports, Science, and Technology (MEXT), Japan and by the JSPS (Japan Society for the Promotion of Science) FIRST program. The first author would like to acknowledge the JSPS for the Research Fellowship for Young Scientists.

REFERENCES

[1] D. A. B. Miller, “Rationale and challenges for optical interconnects to electronic chips,” *Proc. IEEE*, Vol. 88, No. 6, pp. 728-749, June 2000.

[2] D. A. B. Miller, “Device requirements of optical interconnects to silicon chips,” *Proc IEEE*, Vol. 97, No. 7, pp. 1166-1185, July 2009.

[3] S. Matsuo, A. Shinya, Chin-Hui Chen, K. Nozaki, T. Sato, Y. Kawaguchi, H. Taniyama, and M. Notomi, “20-Gbit/s directly modulated photonic crystal nanocavity laser with ultra-low power consumption,” *Optics Express*, Vol. 19, No. 3, pp. 2242-2250, Jan. 2011.

[4] M. Fujita, R. Ushigome, and T. Baba, “Continuous wave lasing in GaInAsP microdisk injection laser with threshold current of 40μA,” *Electron. Lett.*, Vol. 36, No. 9, pp. 790-791, Apr. 2000.

[5] O. Painter, R. K. Lee, A. Scherer, A. Yariv, J. D. O’Brien, P. D. Dapkus, and I. Kim, “Two-dimensional photonic band-gap defect mode laser,” *Science*, Vol. 284, No. 11, pp. 1819-1821, June 1999.

[6] H. G. Park, S. H. Kim, S. H. Kwon, Y. G. Ju, J. K. Yang, J. H. Beak, S. B. Kim, and Y. H. Lee, “Electrically driven single-cell photonic crystal laser,” *Science*, Vol. 305, No. 5689, pp. 1444-1447, Sept. 2004.

[7] T. Okamoto, N. Nunoya, Y. Onoda, T. Yamazaki, S. Tamura, and S. Arai “Optically pumped membrane BH-DFB lasers for low-threshold and single-mode operation,” *IEEE J. Sel. Top. in Quantum Electron.*, Vol. 9, No. 5, pp. 1361-1366, Sept./Oct. 2003.

[8] S. Sakamoto, H. Naitoh, M. Otake, Y. Nishimoto, S. Tamura, T. Maruyama, N. Nishiyama, and S. Arai, “Strongly index-coupled membrane BH-DFB lasers with surface corrugation grating,” *IEEE J. Sel. Top. in Quantum Electron.*, Vol. 13, No. 5, pp. 1135-1141, Sept./Oct. 2007.

[9] K. Oe, Y. Noguchi, and C. Caneau, “GaInAsP lateral current injection lasers on semi-insulating substrates,” *IEEE Photon. Technol. Lett.*, Vol. 6, No. 4, pp. 479-481, Apr. 1994.

[10] T. Okumura, M. Kurokawa, M. Shirao, D. Kondo, H. Ito, N. Nishiyama, T. Maruyama, and S. Arai, “Lateral current injection GaInAsP/InP laser on semi-insulating substrate for membrane-based photonic circuits,” *Opt. Express*, Vol. 17, No. 15, pp. 12564-12570, July 2009.

[11] T. Okumura, H. Ito, D. Kondo, N. Nishiyama, and S. Arai, “Continuous wave operation of thin film lateral current injection lasers grown on semi-insulating InP,” *Jpn. J. Appl. Phys.*, Vol. 49, No. 4, pp. 040205-1-040205-3, Apr. 2010.

[12] T. Okumura, M. Kurokawa, D. Kondo, H. Ito, N. Nishiyama, and S. Arai, “Lateral current injection type GaInAsP/InP DFB lasers on SI-InP substrate,” *The 21st IEEE International Conference on Indium Phosphide and Related Materials (IPRM2009)*, Newport Beach, USA, TuB2 May 2009.

[13] T. Shindo, T. Okumura, H. Ito, T. Koguchi, D. Takahashi, Y. Atsumi, J. H. Kang, R. Osabe, T. Amemiya, N. Nishiyama and S. Arai, “GaInAsP/InP lateral-current-injection distributed feedback laser with a-Si surface grating,” *Optics Express*, Vol. 19, No. 3, pp. 1884-1891, Jan. 2011.

[14] N. Nunoya, M. Nakamura, M. Morshed, S. Tamura, and S. Arai, “High-performance 1.55-μm wavelength GaInAsP-InP distributed-feedback lasers with wirelike active regions,” *IEEE J. Sel. Top. in Quantum Electron.*, Vol. 7, No. 2, pp. 249-258, June 2001.

[15] A. Champagne, R. Maciejko, and T. Makino, “Enhanced carrier injection efficiency from lateral current injection in multiple-quantum-well DFB lasers,” *IEEE Photon. Technol. Lett.*, Vol. 8, No. 6, pp. 749-751, June 1996.